J Therm Spray Tech (2017) 26:661–670
DOI 10.1007/s11666-017-0534-9

PEER REVIEWED

Crack Repair in Aerospace Aluminum Alloy Panels by Cold Spray

P. Cavaliere[1] · **A. Silvello**[1]

Submitted: 4 July 2016 / in revised form: 15 January 2017 / Published online: 7 February 2017

Abstract The cold-spray process has recently been recognized as a very useful tool for repairing metallic sheets, achieving desired adhesion strengths when employing optimal combinations of material process parameters. We present herein the possibility of repairing cracks in aluminum sheets by cold spray. A 2099 aluminum alloy panel with a surface 30° V notch was repaired by cold spraying of 2198 and 7075 aluminum alloy powders. The crack behavior of V-notched sheets subjected to bending loading was studied by finite-element modeling (FEM) and mechanical experiments. The simulations and mechanical results showed good agreement, revealing a remarkable *K* factor reduction, and a consequent reduction in crack nucleation and growth velocity. The results enable prediction of the failure initiation locus in the case of repaired panels subjected to bending loading and deformation. The stress concentration was quantified to show how the residual stress field and failure are affected by the mechanical properties of the sprayed materials and by the geometrical and mechanical properties of the interface. It was demonstrated that the crack resistance increases more than sevenfold in the case of repair using AA2198 and that cold-spray repair can contribute to increased global fatigue life of cracked structures.

Keywords aluminum alloys · cold spray · crack behavior · repairing

✉ P. Cavaliere
pasquale.cavaliere@unisalento.it

[1] Department of Innovation Engineering, University of Salento, Via per Arnesano, 73100 Lecce, Italy

Introduction

Cold spray is emerging as a highly innovative technology for repairing metallic components (Ref 1, 2). Cold spray is suitable for depositing a wide range of traditional and advanced materials on many types of substrate material, especially in nontraditional applications that are sensitive to process temperature (Ref 3). Cold spray can provide different surface modifications leading to increased wear, fatigue, repair, and thermal resistance and heat dissipation by eliminating many of the material incompatibilities common to similar coating technologies (Ref 4). As for all coating technologies, the properties of cold-sprayed materials are primarily dependent on the particle–substrate bonding (Ref 5); the bonding strength is mainly determined by the substrate hardness, powder size and morphology, and spray process parameters (gas temperature, type, and pressure, and nozzle–substrate distance) (Ref 6). Physically, bonding is believed to be governed by shear instability, which leads to bonding enhancement because of melting induced by deformation during nonequilibrium strain. It has been demonstrated that this phenomenon is dependent on an optimal choice of processing parameters (Ref 7). Depending on the materials properties and cold-spray parameters, various interfacial behaviors such as interfacial instability and adiabatic shear instability may be observed, depending on the surface finish, difference between the substrate and particle hardness, and particle impact speed. The gas type, temperature, and pressure, along with the nozzle, control the particle velocity and impact energy. If the energy is too low, particles will not bond to the substrate but rather erode it. Temperature regulates the ductility of the particles and helps them to flatten correctly for bonding. The properties of such coatings also depend on the particle size and

physicomechanical properties of the sprayed material, mechanical properties of the substrate, and processing parameters.

From this point of view, various experimental studies have shown that the microstructure and grain size of the powder greatly influence the properties of the final coating, especially in the case of cold spraying of aluminum alloys (Ref 8, 9). The resulting thermodynamic, kinetic, and solidification models can be used to predict the microstructure and mechanical properties of powder particles.

Processing parameters have a strong effect on the shift in the microstructure from submicrometer to nanocrystalline, which can lead to great improvements in adhesion and mechanical properties (Ref 10). The material deformation mode is governed by the particle speed, which itself depends on the process parameters. For each particle–substrate combination, only a narrow range of processing parameters ensures good deposition efficiency and optimal microstructural and mechanical properties of the sprayed structure.

Also, residual stresses strongly affect the quality of cold-sprayed coatings. They are dependent on the bulk materials. Large particle deformation is experienced if the bulk hardness is higher than the particle hardness. This leads to very high compressive residual stresses in the coating. The residual stresses also depend on the strain due to impact and the thermal mismatch due to the temperature difference between the particles and substrate. When the substrate is softer than the impacting particles, the effect of the thermal mismatch is less pronounced with respect to the strain effect (Ref 11). In some cases, when there is preheating of the carrier gas, a strong effect of thermal mismatch on residual stresses is produced (Ref 12). At the same temperature, higher gas pressures (obtainable in the case of helium) result in higher compressive residual stresses. If high compressive residual stresses are induced at the coating–substrate interface, improved fatigue resistance of cold-sprayed components with respect to the uncoated material is obtained. Fatigue properties are also improved if good adhesion of the coating to the substrate is achieved. In addition, grain refinement due to dynamic recrystallization during impact can delay crack initiation and increase fatigue resistance (Ref 13, 14).

The improved mechanical properties of cold-sprayed coatings are attributed to the surface compressive residual stress state, the good quality of the coatings in terms of no delamination, and surface nanocrystallization that delays crack initiation. From experimental evidence presented in the literature, it is clear that increased fatigue life is achievable if the sprayed particles can produce strong modification of the substrate surface, as in the case of high-pressure deposition. In other cases, the particles cannot produce noticeable modifications, and the tested materials show no change in fatigue properties. The available results, from different authors, show that improved fatigue properties are obtained in coatings characterized by low porosity, high adhesion strength, and high superficial compressive residual stresses. High-pressure cold spray produces coating microstructures characterized by low porosity, optimal splat deformation, high adhesion strength, and high compressive residual stress state. However, even for high-pressure deposition, nonoptimal processing parameters can produce porous coatings with reduced fatigue life. Such coupling between process conditions can also lead to poor coating–substrate adhesion, leading to crack initiation sites at the coating–substrate interphases and decreasing fatigue resistance (Ref 13). In general, cold-sprayed coatings exhibit low fatigue life when cracks initiate at the interface between the coating and substrate because of excessive porosity, low adhesion, or low compressive residual stresses. Very few experimental data on crack initiation and growth behavior of cold-spray coatings have been presented in literature. This lack of data makes it difficult to arrive at conclusive results (Ref 15, 16). Authors who presented lower fatigue results with respect to the base material for 6061 cold-sprayed coatings did not provide the processing details needed to analyze their conclusions (Ref 15). In Ref 17, the results of fatigue crack initiation and growth for 7075 coatings deposited on 2024 aluminum alloy are presented. The authors characterized the specimen's behavior using thermography. Here, strong crack retardation was recorded for the coated samples. The present paper aims to present systematic results on the effect of cold-spray repairing on the crack behavior of aluminum alloy panels.

Experimental Procedures

The chemical composition of the 2099 aluminum alloy of the notched panel and the composition of the cold-sprayed particles are described in Table 1 (wt.%). This alloy was

Table 1 Chemical composition of panel and particle materials employed in the present study

Material	Cu	Li	Zn	Mg	Mn	Zr	Ti	Fe	Si	Cr	Ag	Al
AA2099	2.7	1.8	0.7	0.35	0.35	0.1	0.05	0.05	0.03			Bal.
AA2198	3.2	1.1	0.035	0.6	0.4	0.1	0.05	0.01	0.04	0.05	0.35	Bal.
AA7075	1.5		5.8	2.8	0.25		0.15			0.25		Bal.

developed for use in aerospace and high-strength applications requiring low density, high stiffness, superior damage tolerance, excellent corrosion resistance, and weldability. Alloy 2099 extrusions can replace 2xxx, 6xxx, and 7xxx aluminum alloys in applications such as statically and dynamically loaded fuselage structures, lower wing stringers, and stiffness-dominated designs.

The cold-spray deposits were prepared by using a CGT Kinetics 4000 series cold spray system with a tungsten carbide MOC De Laval nozzle. Argon atomization of vacuum induction-melted nickel ingots using a subsonic argon gas jet (melt nozzle diameter of 50 mm) was used to produce 2198 and 7075 particles. Powders were cooled to room temperature in argon atmosphere. The substrate surface was grit-blasted before deposition. The mean starting particles dimensions were in the range of 5 μm to 60 μm (Fig. 1). The mean grain size of the particles was measured by x-ray diffraction analysis using a Rigaku Ultima+ diffractometer; the values were obtained using the

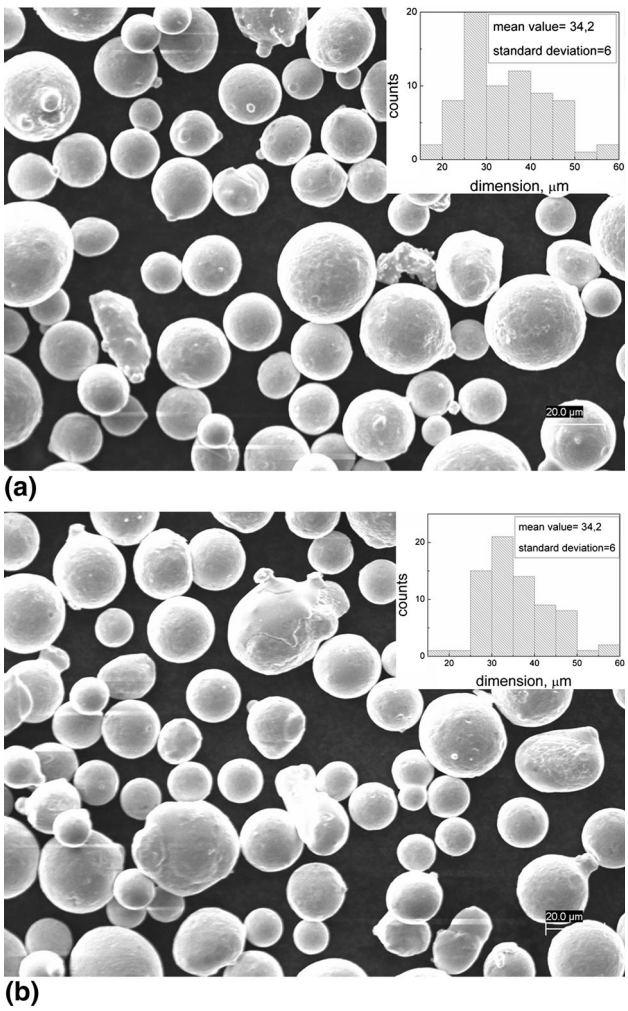

Fig. 1 Aspect and dimensional statistics of 2198 and 7075 particles before spraying

well-known Scherrer equation relating peak broadening to crystallite size using homemade software, as employed in previous studies (Ref 18).

For the 7075 particles, the process gas temperature and pressure were set at 400 °C and 2.5 MPa with stand-off distance of 40 mm. The 2198 particles were sprayed at 450 °C and 2.5 MPa with stand-off distance of 40 mm. A two-dimensional (2D) model of the cold-spray nozzle was employed to analyze the flow field of Ni particles produced by the carrier gas flowing at very high velocities. ANSYS FLUENT commercial software was employed for these simulations. A standard k–ε model was used to take into consideration turbulence due to the high velocity (Ref 19). The calculated particle impact speeds were 900 m/s and 825 m/s, respectively. The coating thickness was around 400 μm. The two alloys were chosen to study the possibility of repairing aluminum panels with the same or a different series, and the efficiency of the process with different materials. The coating microstructure was observed using a Zeiss EVO40 scanning electron microscope. An x-ray Rigaku Ultima+ diffractometer was employed to measure residual stress at coating–substrate interfaces. The hardness, yield strength, and adhesion strength of the coatings were measured by employing a nanoindentation instrument (Micromaterial). Yield stress was measured by nanoindentation, while adhesion strength was measured through nanoscratch tests, all employing a Berkovich indenter (Ref 20).

Using ANSYS, a finite-element code, a three-dimensional (3D) finite-element model was generated, consisting of isoparametric brick elements. The numerical simulations were carried out using appropriate contact elements in ANSYS to model the interface behavior. Cohesive zone models have been used for analysis of structural fracture over the last few years and are highly relevant in problems for which the key physical processes involved in the fracture event take place over a very narrow region. The cohesive zone model consists of a constitutive relation between the traction acting on the interface and the corresponding interface separation representing the displacement jump across the interface (Ref 21). The constitutive relationship between the cohesive stress and the shear separation is experimentally determined. The interface surfaces of the materials can be represented by a special set of interface elements or contact elements, and a cohesive zone model (CZM) can be used to characterize the constitutive behavior of the interface. In the CZM, fracture is treated as a gradual phenomenon in which separation resisted by cohesive traction takes place across a cohesive zone. The extension of this cohesive zone ahead of the crack tip is modeled using traction–separation laws (also known as a cohesive law) relating the cohesive stress to the separation in the process zone. The interface surfaces of the

materials can be represented by a special set of interface elements or contact elements, and a CZM model can be used to characterize the constitutive behavior of the interface. Three-dimensional elements CONTA174 and TARGE170 were used to simulate interface separation. They possess the capacity to model the separation of a bonded contact by using the TB command with the CZM (cohesive zone model) label. The bilinear cohesive zone model is available in ANSYS. There are two ways to specify the interface parameters: bilinear interface behavior with tractions and separation distances (TB, CZM command with TBOPT = CBDD) or bilinear material behavior with tractions and critical fracture energies (TB, CZM command with TBOPT = CBDE) (Ref 22, 23). Three-phase unit cells with hexagonal symmetry were employed.

Crack growth tests were performed by employing an Instron 8801 servohydraulic machine. The specimens were tested in (three-point) bending with load direction perpendicular to the coating surface. The specimens measured 50 mm × 20 mm × 5 mm. The distance between the supporting pins was 30 mm. The tests were performed at room temperature using a sinusoidal waveform at loading frequency of 20 Hz under constant-amplitude loading with load ratio $R = 0.1$ [E1290: Standard Test Method for Crack-Tip Opening Displacement (CTOD) Fracture Toughness Measurement]. Crack growth was monitored using a direct-current potential drop method (Ref 24). Obviously, the crack-tip plasticity and crack initiation and growth behavior depend on the crack geometry, and a machined crack will always differ from a crack that forms in use. In the authors' opinion, the repair is strongly influenced by the crack geometry; further research (already in process) will focus on the variation of the crack initiation and growth with the crack geometry, for example, the V-notch angle.

Results and Discussion

The 2099 aluminum alloy panel was 2 mm thick with area of 20 mm × 20 mm. A 30° notch with height of 100 μm was machined at the center of the panel (Fig. 2), then the

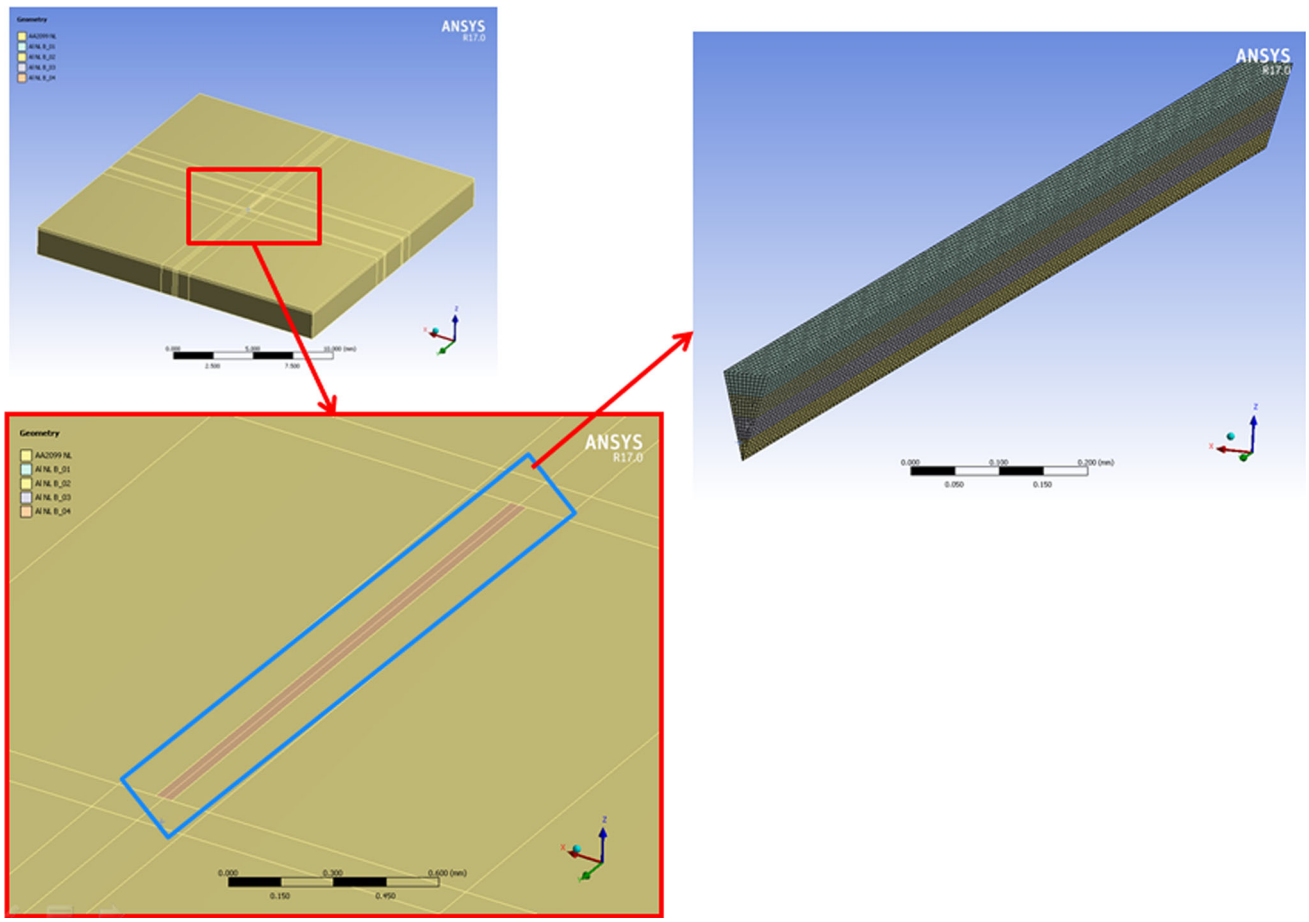

Fig. 2 Panel with 30° V notch in center

surfaces were grit-blasted before spraying (Fig. 3). The mechanical properties of the AA2099 sheet are reported in Table 2.

The grain size of the 2198 and 7075 aluminum alloy particles was measured to be 1.2 ± 0.1 mm and 1.4 ± 0.1 mm, respectively.

The panel notch was filled with 7075 and 2198 aluminum alloy particles via cold spray, and samples were cut (by FIB, Hitachi FB-2000A) parallel to the coating–substrate interface to perform adhesion strength measurements.

The microstructure of the 2198 coating sprayed at 450 °C and 2.5 MPa is shown in Fig. 4.

The cold-spray coatings were characterized by measuring the shear bond strength as a function of distance from the crack tip, shown in Fig. 5 for both the 2198 and 7075 cold-sprayed coatings.

The variation of the yield strength of the coating materials, as a function of the crack tip–surface distance, is shown in Fig. 6.

The measured residual stresses for both coatings, as a function of the distance from the surface, are shown in Fig. 7.

The maximum principal stress and the total deformation of the repaired material are shown in Fig. 8 for the case of the 2198 cold-sprayed panel.

Repairing the crack with a cold-sprayed coating caused a notable change in the principal stresses (Fig. 8). Figure 9 reports the relative values of maximum principal stresses at the same point within the 2099 bulk, obtained by ratioing the results obtained before (σ_{max} 2099) and after (σ_{max} 2209–7075 or –2198) crack repair. It should be underlined that: (1) with an open crack, the stress intensity factor is maximum at the crack tip then decreases along the side towards the sheet surface; (2) on the contrary, in the case of a cold-sprayed sealed crack, it exhibits its minimum at the crack tip then increases towards the sheet surface.

This is due to the coupling of the increase of the panel strength due to the presence of the coating material and to

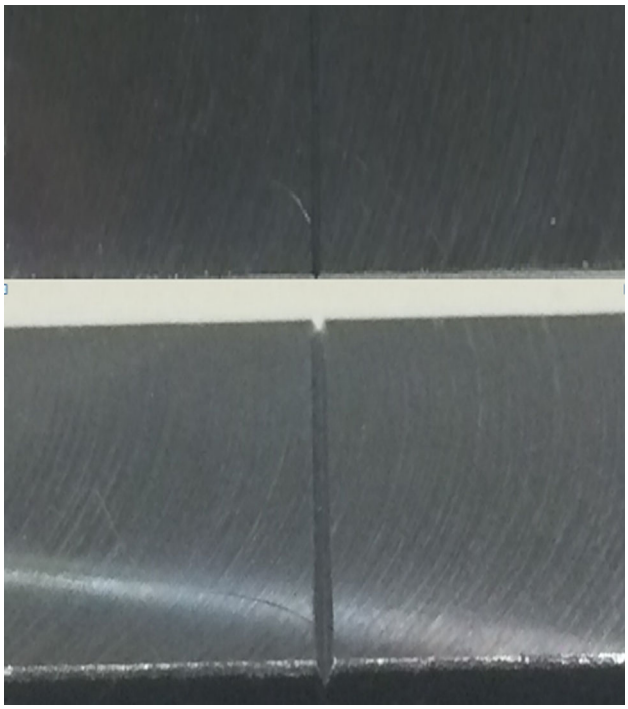

Fig. 3 Machined notch in aluminum panels

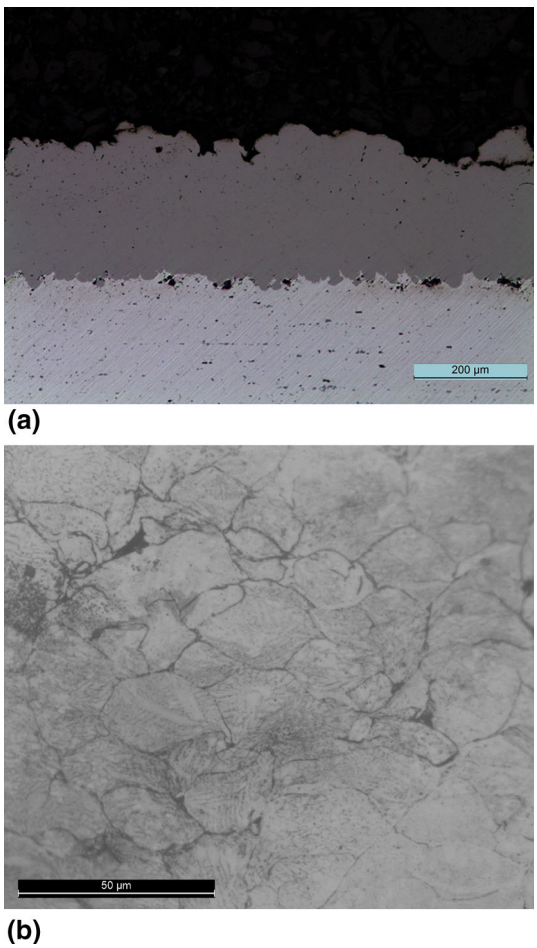

Fig. 4 Microstructure of 2198 coating spayed at 450 °C and 2.5 MPa

Table 2 Mechanical properties of 2099 sheet of present study (Ref 17)

Material	*E*, GPa	YS, MPa	UTS, MPa	El., %	Fatigue limit, MPa	K_{IC}, MPa $m^{-1/2}$
AA2099	75	430	530	10	175	55

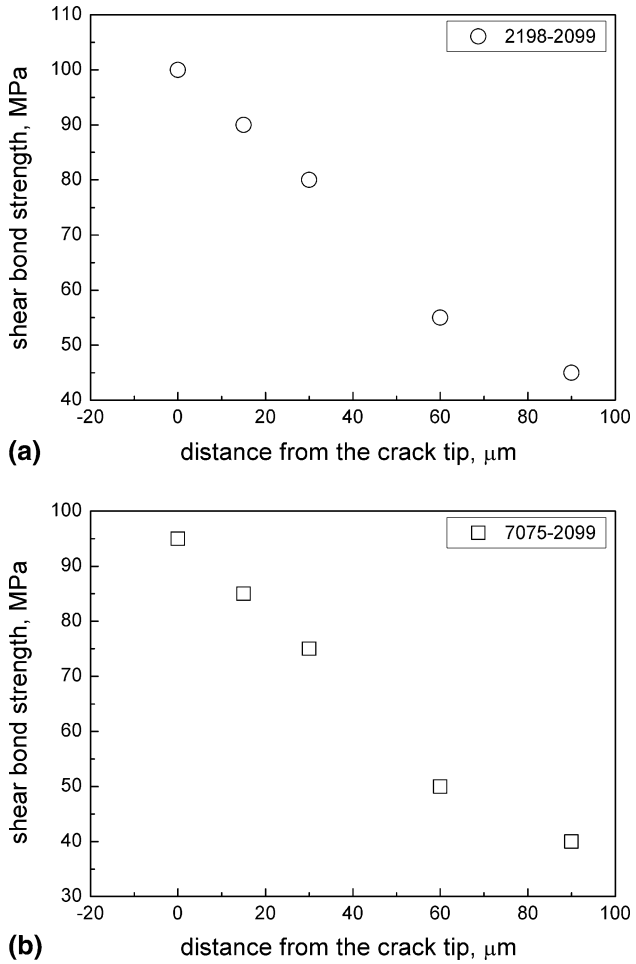

Fig. 5 Shear bond strength for 2198 and 7075 cold-sprayed coatings as function of crack tip–surface distance

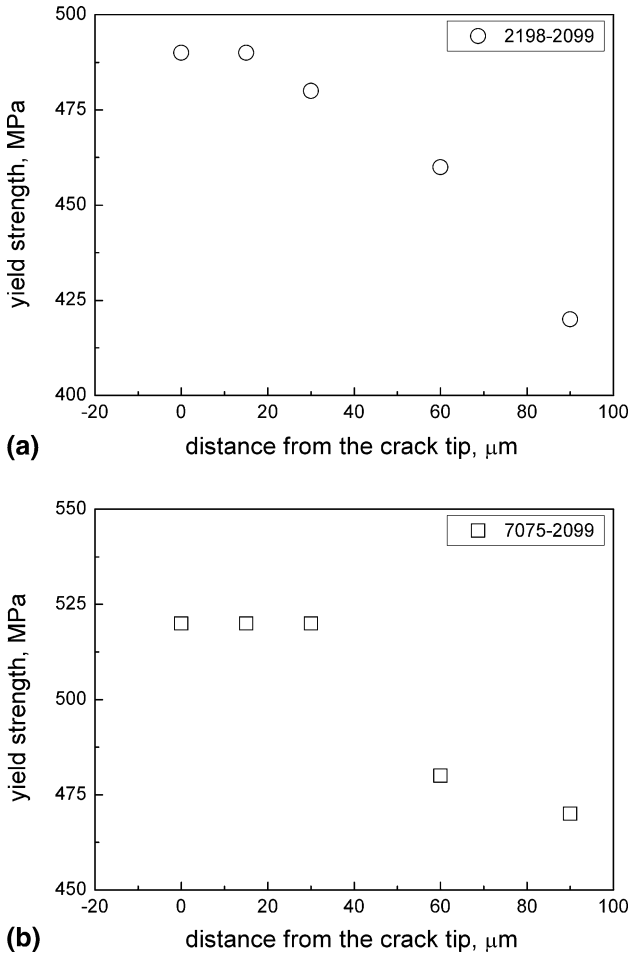

Fig. 6 Yield strength for 2198 and 7075 cold-sprayed particles as function of crack tip–surface distance

the size and shape of the plastic zone leading to crack growth retardation.

In Fig. 10, the crack length as a function of the number of loading cycles is plotted for the panels repaired with AA2198 and AA7075 coatings; for comparison, the same data for the unrepaired panels is also reported.

The crack resistance of the repaired panels was increased sixfold in the case of 7075 coatings and more than sevenfold in the case of repair with AA2198 coating. This demonstrates that cold-spray repair can greatly contribute to increase the global fatigue life of cracked structures. It is believed that fatigue resistance is strongly increased as the adhesion strength of the coating to the panel is increased; the better the cold-sprayed material adheres to the bulk, the more the onset of crack initiation and growth is delayed. Adhesive disbond over the crack region can significantly reduce stress transfer between the repaired plate and the coating, producing a strong drop in repair efficiency. The residual stresses at the interfaces strongly affect the crack behavior. Higher particle velocity

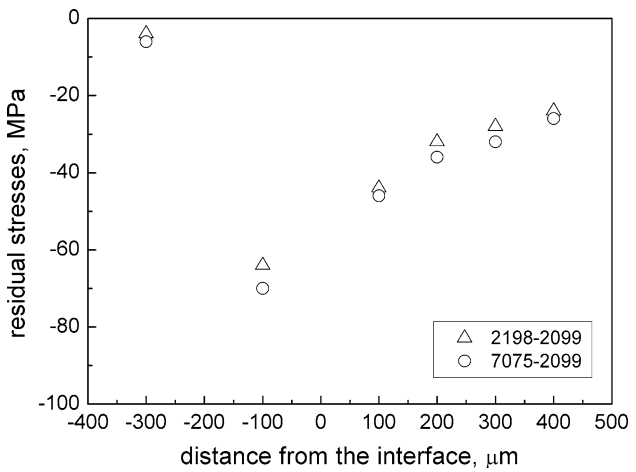

Fig. 7 Residual stresses for both the 2198 and 7075 coatings

results in improved adhesion strength because of increased impact temperature and deformation. Particle–substrate bonding is a combination of different mechanisms. The

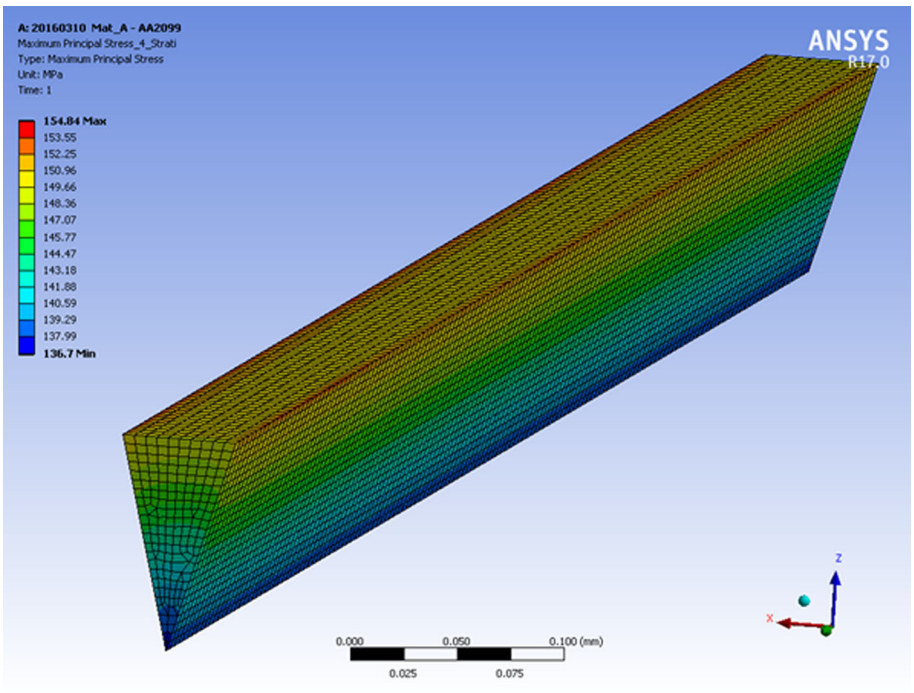

(a)

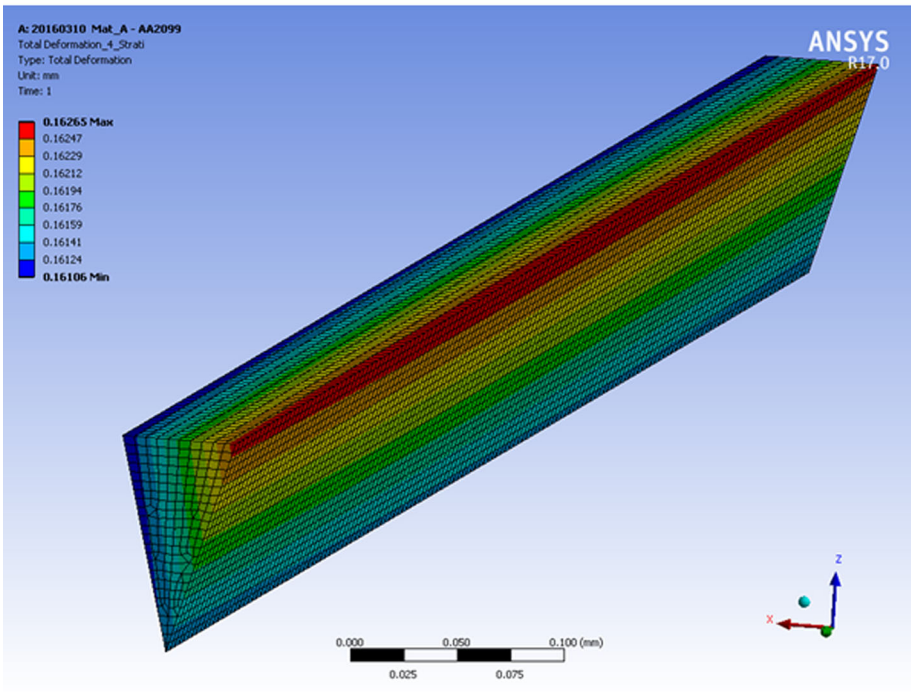

(b)

Fig. 8 Maximum principal stress (a) and total deformation (b) for the 2099 panel repaired with 2198 coating via cold spray

localized bonding is due to localized impact fusion; in addition, bonding is also due to metal–metal bonding, mechanical locking, and diffusion. Metal–metal locking and mechanical bonding increase with increasing particle velocity, while diffusion bonding is amplified by temperature increase (Ref 25, 26). Optimal deformation of the coating material has been identified as the main factor producing adhesion strength in coatings (Ref 27). In addition, such adhesion strength levels are due to the small number of voids observed at the coating–substrate interface. The porosity is strongly dependent on the sprayed material and processing parameters. During impact,

particles flatten and assume a pancake-like structure characterized by high flattening ratio. If the plastic deformation is insufficient, particles retain their original spherical shape, which leads to higher porosity levels in the coatings. High porosity levels can affect the fatigue behavior if a large amount of pores is concentrated at the coating–substrate interface. Further research is needed to better understand the fatigue resistance and crack behavior of cold-spray coatings. In this kind of application, the optimal processing parameters must be tuned as a function of the sprayed particles to achieve the best mechanical and microstructural properties of the coatings. It is reported in literature (Ref 11) that residual stresses depend on the strain effect due to the impact and thermal mismatch due to the temperature difference between the particles and substrate. In the case of a softer substrate, the effect of thermal mismatch is much less pronounced with respect to the strain effect. Experiments on preheated substrates show that preheating has a strong effect on the thermal mismatch and on the residual stresses when very high pressures are employed during spraying (Ref 12). The crack growth rate as a function of the applied ΔK for all the tested panels is shown in Fig. 11.

To investigate the possibility of increasing the repairing efficiency by achieving improved fatigue performance using higher-quality cold-spray deposits, 2198 aluminum alloy was cold sprayed at lower temperature and pressure (350 °C and 1.5 MPa). In particular, such conditions lead to a strong reduction in the adhesion strength and an increase in the porosity compared with previously employed processing conditions (Ref 3). The microstructure of coatings sprayed at 350 °C and 1.5 MPa is shown in Fig. 12. Decreased fatigue resistance is observed when employing processing conditions that result in decreased adhesion strength (Fig. 13). In particular, very fast crack growth is revealed, with behavior in zones II and III that becomes very similar to that of the unrepaired panel.

The fatigue resistance is strongly related to the coating–panel disbond. Efficient crack repair using the cold-spray technique requires close attention to the deposition conditions leading to optimal microstructural properties of the coatings. In addition, the increased elastic modulus in the case of low-porosity cold-sprayed coatings is believed to make such structures sensitive to deformation-induced cracking (Ref 28). If high-pressure cold-spray equipment is employed, high levels of superficial compressive stress are measured in cold-sprayed samples. In fact, the improved fatigue resistance with respect to the uncoated material is due to compressive residual stresses induced by the process, and to the good adhesion of the coating to the substrate. In addition, dynamic recrystallization, due to severe plastic deformation of the particles impacting on the

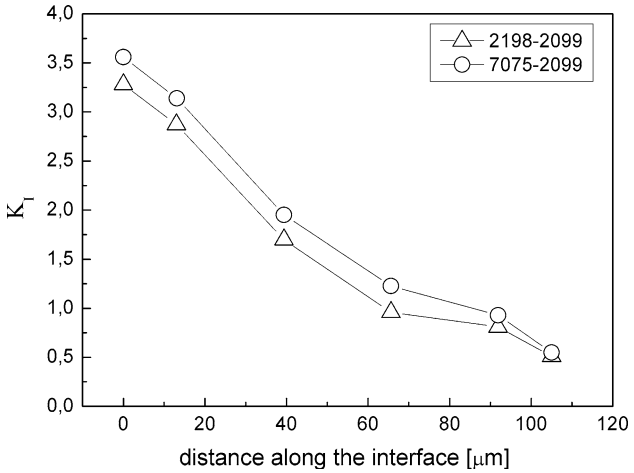

Fig. 9 Maximum principal stress ratio between cracked and repaired panels

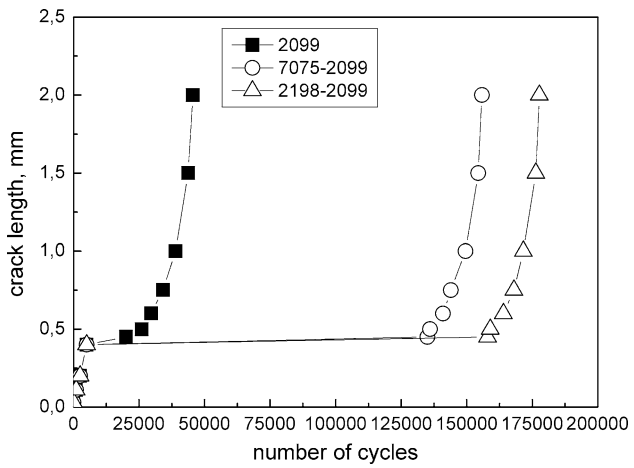

Fig. 10 Crack length as function of number of loading cycles for all tested panels

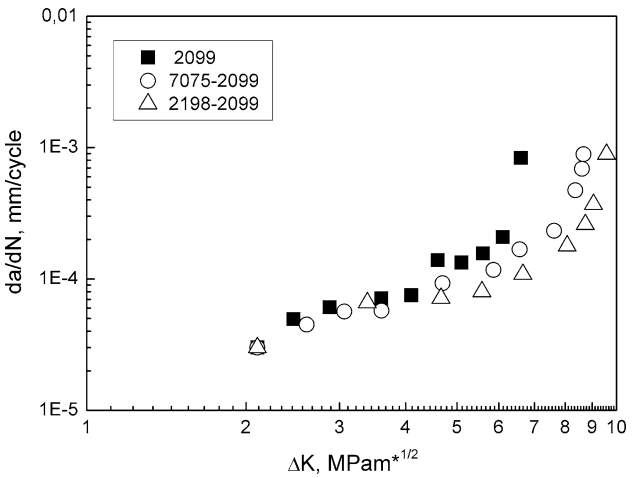

Fig. 11 Crack growth rate as function of applied ΔK for all tested panels

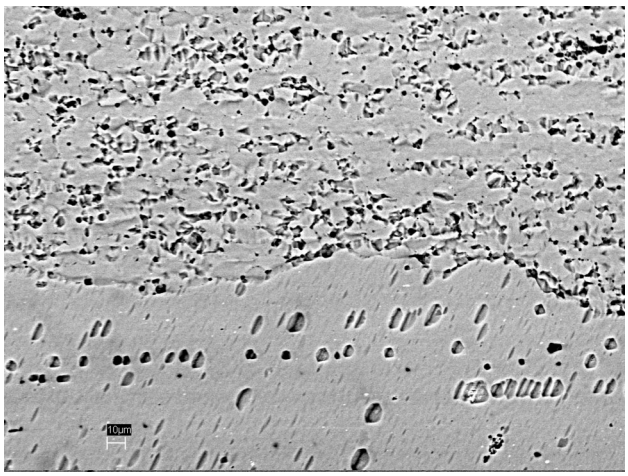

Fig. 12 2198 aluminum alloy cold sprayed at 350 °C and 1.5 MPa

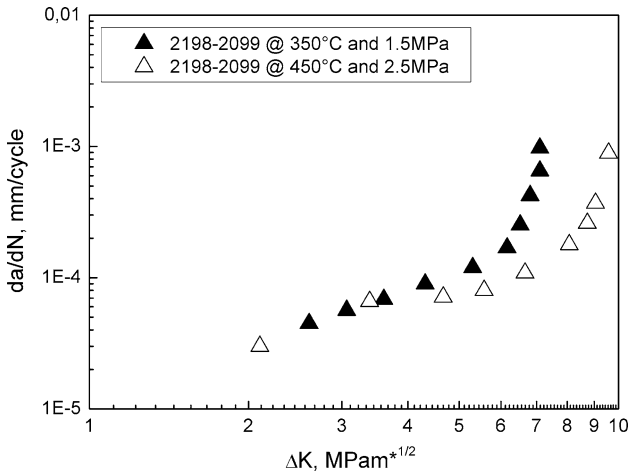

Fig. 13 Crack growth rate of cold-sprayed 2198 alloy on 2099 panel, employing different processing conditions

surface, produces optimal microstructures resulting in crack initiation delay. It is reported in literature (Ref 11) that the residual stresses depend on the strain effect due to the impact and the thermal mismatch due to the temperature difference between the particles and substrate. In the case of a softer bulk, the thermal mismatch effect is much less pronounced with respect to the strain effect. As an additional demonstration, some experiments performed on preheated substrates showed that, over some temperature range, preheating leads to a stronger effect of thermal mismatch on residual stresses also in the case of employing very high pressures during spray (Ref 12). In this case, all the cracks initiate at the coating–substrate interface, making the adhesion conditions fundamental for increasing the fatigue life. It is reported in literature that the intercrystalline crack propagation mechanism is dominant in cold-spray specimens (Ref 29). Actually, the adhesion strength depends on the spraying conditions. Particles sprayed at higher gas preheating temperatures are expected to retain some thermal energy and arrive at the substrate at higher temperature than those with lower gas preheating temperatures. In terms of cold-spray coatings, it is important to note that the gas temperature will increase the substrate temperature. Higher particle velocity results in improved adhesion strength because of the increase in impact temperature and deformation. Particle–substrate bonding is a combination of different mechanisms. The localized bonding is due to localized impact fusion; in addition bonding is also due to metal–metal bonding, mechanical locking, and diffusion. Metal–metal locking and mechanical bonding increase with increasing particle velocity, while diffusion bonding is amplified by temperature increase (Ref 25, 26). In general, the optimal deformation of the coating material is indicated as the main factor leading to strong adhesion strength of coatings.

Conclusions

The present study aimed to analyze the potential of cold-spray technology for crack repair to obtain an increase in precracked panel tolerance to crack initiation and growth. A surface V-notch with 30° aperture was produced in a 2099 aluminum alloy panel and repaired with 2198 and 7075 alloys via cold spray. ANSYS finite-element calculations demonstrated that the locus of crack initiation moved toward the surface in the repaired panels. Crack initiation and growth tests revealed that the repaired panels had up to sixfold crack resistance when optimal processing parameters were used. The fatigue resistance of the panels was related to the microstructural quality of the coatings. In particular, if nonoptimal processing parameters were employed (350 °C and 1.5 MPa), decreased adhesion strength and increased coating porosity were recorded; in this case, a strong drop in crack resistance was observed compared with coatings produced using optimal process parameters (450 °C and 2.5 MPa).

References

1. V.K. Champagne and P.F. Leyman, Repair of apache mast support on AH64 helicopter using cold spray. In: Failure Prevention for System Availability—Proceedings of the 62nd Meeting of the Society for Machinery Failure Prevention Technology.
2. K. Ogawa and T. Niki, Repairing of Degraded Hot Section Parts of Gas Turbines by Cold Spraying, *Key Eng. Mater.*, 2010, **417–418**, p 545-548
3. P. Cavaliere and A. Silvello, Processing Parameters Affecting Cold Spay Coatings Performances, *Int. J. Adv. Manuf. Technol.*, 2014, **71**, p 263-277

4. A. Sova, S. Grigoriev, A. Okunkova, and I. Smurov, Potential of Cold Gas Dynamic Spray as Additive Manufacturing Technology, *Int. J. Adv. Manuf. Technol.*, 2013, **69**, p 2269-2278
5. H. Assadi, F. Gärtner, T. Stoltenhoff, and H. Kreye, Bonding Mechanism in Cold Gas Spraying, *Acta Mater.*, 2003, **51**, p 4379-4394
6. T. Schmidt, F. Gärtner, H. Assadi, and H. Kreye, Development of a Generalized Parameter Window for Cold Spray Deposition, *Acta Mater.*, 2006, **54**, p 729-742
7. S.V. Klinkov, V.F. Kosarev, and M. Rein, Cold Spray Deposition: Significance of Particle Impact Phenomena, *Aerosp. Sci. Technol.*, 2005, **9**, p 582-591
8. D. Cote, V. Champagne, and R.D. Sisson, Computational Through-process Modeling for Cold Sprayed Alloy Optimization. In: Materials Science of Additive Manufacturing-Proceedings of Materials Science and Technology 2014.
9. B. McNally, Experimental Verification of Through-Process Modeling of Cold Spray Al Alloys. In: AeroMat 2015 Conference and Exposition.
10. L. Ajdelsztajn, B. Jodoin, and J.M. Schoenung, Synthesis and Mechanical Properties of Nanocrystalline Ni Coatings Produced by Cold Gas Dynamic Spraying, *Surf. Coat. Technol.*, 2006, **201**, p 1166-1172
11. K. Spencer, V. Luzin, N. Matthews, and M.-X. Zhang, Residual Stresses in Cold Spray Al Coatings: The Effect Of Alloying and of Process Parameters, *Surf. Coat. Technol.*, 2012, **206**, p 4249-4255
12. S. Rech, A. Trentin, S. Vezzú, J.G. Legoux, E. Irissou, and M. Guagliano, Influence of Pre-heated Al 6061 Substrate Temperature on the Residual Stresses of Multipass Al Coatings Deposited by Cold Spray, *J. Therm. Spray Technol.*, 2011, **20**(1–2), p 243-251
13. P. Cavaliere and A. Silvello, Processing Conditions Affecting Residual Stresses and Fatigue Properties of Cold Spray Deposits, *Int. J. Adv. Manuf. Technol.*, 2015, **81**, p 1857-1862
14. P. Cavaliere and A. Silvello, Fatigue Behaviour of Cold Sprayed Metals and Alloys: Critical Review, *Surf. Eng.*, 2016, **32**(9), p 631-640
15. A.G. Gavras, B.F. Chenelle, and D.A. Lados, Effects of Microstructure on the Fatigue Crack Growth Behavior of Light Metals and Design Considerations, *Rev. Mater.*, 2010, **15**(2), p 319-329
16. R. Jones, M. Krishnapillai, K. Cairns, and N. Matthews, Application of Infrared Thermography to Study Crack Growth and Fatigue Life Extension Procedures, *Fat. Fract. Eng. Mater. Struct.*, 2010, **33**, p 871-884
17. B. Bozzini, P. Cavaliere, I. Sgura, and C. Mele, Crack Repairing in AA2099 by Cu Electrodeposition (ECD), Crack Path 2012, Gaeta, Italy, September 19–21 2012, pp. 603–601
18. P. Cavaliere, A. Perrone, and A. Silvello, Multi-objective Optimization of Steel Nitriding, *Eng. Sci. Technol.*, 2016, **19**, p 292-312
19. F.R. Menter, M. Kuntz, and R. Langtry, Ten Years of Industrial Experience with the SST Turbulence Model, *Turbul. Heat Mass Transf.*, 2003, **4**, p 625-632
20. R.R. Chromik, D. Goldbaum, J.M. Shockley, S. Yue, E. Irissou, J.G. Legoux, and N.X. Randall, Modified Ball Bond Shear Test for Determination of Adhesion Strength of Cold Spray Splats, *Surf. Coat. Technol.*, 2010, **205**, p 1409-1414
21. A. Beakou and K. Charlet, Mechanical Properties of Interfaces Within a Flax Bundle—Part II: Numerical Analysis, *Int. J. Adhes. Adhes.*, 2013, **43**, p 54-59
22. ANSYS13.0. ANSYS user manual. http://148.204.81.206/Ansys/150/ANSYS%20Mechanical%20Users%20Guide.pdf, 2012
23. A. Turon, C.G. Davila, P.P. Camanho, and J. Costa, An Engineering Solution for Mesh Size Effects in the Simulation of Delamination Using Cohesive Zone Models, *Eng. Fract. Mech.*, 2007, **74**(10), p 1665-1682
24. P. Cavaliere, Fatigue Properties and Crack Behavior of Ultra-Fine and Nanocrystalline Pure Metals, *Int. J. Fatigue*, 2009, **31**, p 1476-1489
25. Q. Wang, N. Birbilis, and M.-X. Zhang, On the Formation of a Diffusion Bond from Cold-Spray Coatings, *Met. Trans.*, 2012, **A43**(5), p 1395-1399
26. H.X. Hu, S.L. Jiang, Y.S. Tao, T.Y. Xiong, and Y.G. Zheng, Cavitation Erosion and Jet Impingement Erosion Mechanism of Cold Sprayed Ni–Al_2O_3 Coating, *Nucl. Eng. Des.*, 2011, **241**, p 4929-4937
27. R. Ghelichi, S. Bagherifard, D. Mac Donald, M. Brochu, H. Jahed, B. Jodoin, and M. Guagliano, Fatigue Strength of Al Alloy Cold Sprayed with Nanocrystalline Powders, *Int. J. Fatig.*, 2014, **61**, p 51-57
28. F. Kroupa, Nonlinear Behavior in Compression and Tension of Thermally Sprayed Ceramic Coatings, *J. Therm. Spray Technol.*, 2007, **16**, p 84-95
29. A. Moridi, S.M. Hassani-Gangaraj, S. Vezzú, L. Trško, and M. Guagliano, Fatigue Behavior of Cold Spray Coatings: The Effect of Conventional and Severe Shot Peening as Pre-/Post-treatment, *Surf. Coat. Technol.*, 2015, **283**, p 247-254